INTERNATIONAL ATOMIC ENERGY AGENCY
UNITED NATIONS EDUCATIONAL, SCIENTIFIC AND CULTURAL ORGANIZATION

INTERNATIONAL CENTRE FOR THEORETICAL PHYSICS
34100 TRIESTE (ITALY) - P.O.B. 586 - MIRAMARE - STRADA COSTIERA 11 - TELEPHONE: 2240-1
CABLE: CENTRATOM - TELEX 460392 - I

SMR/382- 9

WORKSHOP ON SPACE PHYSICS:
"Materials in Micorgravity"
27 February - 17 March 1989

"On the Effects of in Orbit Accelerations on Microgravity Experiments in Fluid Dynamics"

R. MONTI
University of Naples
Institute of Aerodynamics "U. Nobile"
Naples, Italy

ON THE EFFECTS OF IN ORBIT ACCELERATIONSON MICROGRAVITY EXPERIMENTS IN FLUIDYNAMICS

R.Monti - C.Golia
Istituto di Aerodinamica "Umberto Nobile"
Universita' di Napoli

Summary

The effects produced by the various types of g-disturbances occurring during manned space missions in fluid science microgravity experiments are evaluated through extenxive numerical experimentations with a code solving the full set of Navier-Stokes Equations.

Parameter norms to measure the fluid and the thermal disturbance effects, and new criteria are then proposed for the evaluation of the maximum acceptable g-fields on microgravity platforms for fluid experiments in terms of the various typologies of the g-jitters.

1. INTRODUCTION

Microgravity experimentations on space platforms are obviously motivated by the need of a quiet, very low g-environment. An ideal Microgravity Environment (MG) is a real zero-g that does not appear feasible in LEO Spacecrafts mainly because of the air drag, S/C manouvres, rotating machinery on boards, and, when present, crew activity.

Latest recording on the g-field on board of manned dedicated missions show how g-disturbances of random nature (g-jitters) exhibit relatively large peaks (of the order of 10 g) that may affect a number of microgravity experiments.

The evaluation of the effects of those g-disturbances on different classes of experiments is of paramount importance for the experimenters, for the payloads manufacturing companies and for the Space Agencies that must specify the requirements on the "allowable" g-levels (or g-fields) for the S/C on which the Microgravity Experiment takes place.

Following the work reported in [6] we review the previous criteria of the allowable g-levels (e.g. as specified by ESA for unmanned platforms like EURECA) and

to demonstrate, on the basis of an extensive numerical experimentation made by codes solving the complete Navier-Stokes Equations, what is the effect of the various types of the g-disturbances (steady state, periodic or pulsed with different time profiles), what is the best norm to measure the effects caused by such disturbance, and how to define criteria for the evaluation of the limit accettable disturbances.

The cases simulated by the numerical codes refer to the ThermoFluidynamic fields established during a typical crystal growth from solution in MG, in presence of the above g-disturbances.

Preliminary conditions are drawn and new criteria are proposed for the requirements of the "maximum acceptable" g-fields on microgravity platforms, for each type of disturbances.

2. ANALYSIS OF THE MICROGRAVITY LEVELS

It is quite surprising to note that the planning of several space programs in the contest of Microgravity Sciences (Material/Fluid) has been done without a deep analysis of the levels and of the quality of the gravitational and acceleration fields actually attainable on board of the S/C.

The acceleration level in space platforms is obviously of several order of magnitude smaller than the ground level but sporadic measurements during the manned Spacelab and Salyut missions [1] had reported a rather frequent occurrence of relatively large g-peaks.

A very careful analysis of these g-disturbances is then necessary to set up the g-disturbance scenario.

Up to now all the planning of MG activities has been based on the "g-level versus frequency" plots reccomended for the US Space Stations reported in Fig.1 and for other platforms (e.g. EURECA).

The measurements taken in the D-1 Spacelab Mission and reported by Hamaker et alia in [2] are the most recent and valid contribution to clarify and to define the acceleration microgravity scenario.

The acceleration field $\underline{A}$ on board of a spacecraft can be characterized as a sum of two contributions:

$$\underline{A} = \underline{A}s + \underline{A}j$$

2.2 Transient Accelerations

Measurement taKen on the DI mission, that must be recognized as the first space microgravity dedicated mission, has allowed, for the first time, to correlate g-disturbances with their causes.

The transient accelerations (also referred to as "g-jitters") present a quite wide range of typology and can be broadly classified as external and internal g-jitters.

2.2.1 External Induced Disturbances

Transient external forces may result from operational activities (i.e. thruster firings) and extravehicular activities. They induce, in general, also a torque resulting in a transient rotational acceleration phase followed by a quasi steady acceleration due to rotation around the CM.

The order of magnitude of such disturbances depends on the two thruster system fired.

The Vernier Thruster System (VRCS) has been identified as responsable for spiKes of the order of 10^{-3} g_o. The frequency of attitude manovres depends much on the mission. In a MG oriented mission the orbiter is flown most of the time in a gravity gradient stabilized mode with time phases lasting from 7 to 12 hours each.

The Primary Thrusters (PRCS) , utilized for velocity changes (orbit corrections) have caused spiKes up to 60 [mg_o] and a long decay time (about 11 [s]). Their firing is quite rare in MG phase of the misions.

2.2.2 Internal Induced Disturbances

The internal motion of mechanical parts, crew activities, sled experiments etc. cause variations of the mass allocation inside the S/C without causing variation of its total momentum.

Such disturbances generated by internal causes are always compensated by opposite impulses after a time delay.

Sled tipe experiment in DI caused spiKes up to 2.4 mg_o at a frequency of 5 Hz (that correspond to the eigen-frequency of the Spacelab Module.

The handling activities of MSDR induced spiKes of the order of 7 mg_o, whereas their operational activity

caused spiKes of 3 mg_o.

Crew activity have been identified (from a detailed analysis of video tapes) as causing spiKes up to 10 mg_o (closig of the ceiling door) and spiKes of 2-3 mg_o for normal closed-by activity and handling.

The "quiet phase" was monitored to present spiKes smaller than 0.3 mg_o.

2.3 The assumed MG scenario.

All the MG levels measured in the DI are plotted in Fig.1 and compared with the NASA recommended limits for the Space Stations (similar to the ones for EURECA)

The analysis of all these data, and of their comparison with the Soviet mission data, show that the g-jitters caused by Crew Motion are one order of magnitude higher than the level expected by NASA.

In setting a scenario for the MG levels the following comments apply:

-Quasi Steady Accelerations-

Their predicted level (10^{-6} g_o) is confirmed, they can be minimized (by allocating the MG Facilities close by to CM) but cannot be eliminated.

-Transient Accelerations-

They have different order of magnitude. Their number can be minimized by suitable planning of the MG segment, but the emerging point is that the disturbances caused by crew activity is larger than predicted (2-3 mg_o) and that the "quite phase" still present spiKes of 0.3 mg_o.

The typology and quality of the disturbance deserve a detailed discussion.

The harmonic disturbance are correlated mainly to the vibrational characteristics of the S/C structures.

But many other disturbances are most frequent and important ,these are mainly represented by single pulses (deriving from external causes) or by couple of inverse pulses (from internal causes).

For disturbances having this typology no analysis has been done up to day, nor criteria are available to ascertain their allowable limits.

3. THERMOFLUIDYNAMIC MODELLING

The geometry considered sketched in Fig.2 consider the simulation of a crystal growth (from solution) experiment, that is quite critical in terms of g-tollerability.

This refer to a liquid specimen that fills a cylindrical container (radius R, length L) whose boundaries are mantained at a constant temperature Tb.

A crystal seed is located at the center of the cylinder, and is kept at a constant temperature Tb.

In presence of a zero gravity condition (g=0) a purely diffusive temperature steady state conditions are established that correspond to a quiescent flow regime.

In presence of g-levels (either residual gravity or g-jitter) the flow and the temperature fields are distorted because of the induced convection caused by buoyant forces.

The time evolution of the disturbances, as compared with the zero gravity quiescent state, are analized together with the relaxation process that takes place after the disturbance.

3.1 Formulation of the problem

By assuming:

i) Newtonian, non micropolar, single componet fluid;
ii) Variable transport properties;
iii) Boussinesque approximation for the density;
iv) Axisymmetric flow and temperature fields;

the non dimensional full Navier-Stokes equations can be expressed in terms of the vorticity $\underline{\zeta}$, of the temperature ϑ, of the stream function ψ, and of the pressure π, as follows:

$$Pe\left[Str\frac{\partial\vartheta}{\partial\tau}+\underline{\nabla}\cdot(\underline{V}\vartheta)\right]=\lambda\nabla^2\vartheta+\underline{\nabla}\vartheta\cdot\underline{\nabla}\lambda+PrEc\mu(\underline{\nabla}\underline{\nabla}):(\underline{\nabla}\underline{V})^S \qquad (1)$$

$$Re\left[Str\frac{\partial\underline{\zeta}}{\partial\tau}-\underline{\zeta}\cdot\underline{\nabla}\underline{V}+\underline{V}\cdot\underline{\nabla}\underline{\zeta}\right]= Gr\,\underline{i}_g\wedge\underline{\nabla}\vartheta+\mu\nabla^2\underline{\zeta}+\underline{\nabla}\mu\wedge\nabla^2\underline{V}+\underline{\nabla}\wedge[2\underline{\nabla}\mu\cdot(\underline{\nabla}\underline{\zeta})] \qquad (2)$$

$$\underline{\zeta}=\underline{\nabla}\wedge[\underline{\nabla}\wedge(\psi\,\underline{i}_\vartheta/h_\vartheta)] \qquad (3)$$

$$\nabla^2\pi=-Re(\underline{\nabla}\underline{V}):(\underline{\nabla}\underline{V})-Gr\,\underline{i}_g\cdot\underline{\nabla}\vartheta \qquad (4)$$

These equations are respectively the energy balance (with viscous dissipation), the curl of the momentum balance equation, the equation defining the vorticity in terms of the stream function, and the Poisson's equation for the pressure, where:

- $Re = Vr\,Lr/\nu r$ is the Reynolds number;
- $Str = tr\,Vr/Lr$ is the Strouhal number;
- $Gr = g\beta_T(\Delta T)\,Lr/Vr^2$ is the Grashoff number;
- $Pr = \nu_2/a_4$ is the Prandtl number;
- $Ec = Vr^2/Cp\,(\Delta T)$ is the Eckert number;
- $Pe = Re\,Pr$ is the Peclet number;
- $\vartheta = (T-Tb)/(Ts-Tb)$ is the nondimensional temperature;
- $\underline{V} = \underline{\nabla}\wedge(\psi\,\underline{i}_\vartheta/h_\vartheta)$ is the nondimensional velocity;
- π = the pressure (with respect to the quiescent state) normalized to the viscous stress ($\mu_2 Vr/Lr$)
- $\underline{i}_\vartheta$ and h_ϑ are respectively the unit vector normal to the plane of motion and its metric coefficient;
- $(\Delta T) = (Ts-Tb)$ is the reference temperature difference;
- $\tau = t/tr$ is the non dimensional time
- $\lambda = \lambda(T)/\lambda(Tb)$ is the the thermal conductivity referred to its value at the boundary;
- $\mu = \mu(T)/\mu(Tb)$ is the dynamic viscosity referred to its value at the boundary.

The spatial coordinates are referred to the cylinder height L, so that the computational mesh lays within :

$$0 \leq X \leq 1 \quad ; \quad 0 \leq Y \leq R/L$$

Boundary conditions are no slip and assigned temperature ($\vartheta=0$) on the cylinder walls, and symmetry conditions around the centerline.

Temperature is assigned ($\vartheta=1$) on the seed's wall, that is descritized for the thermal field as a small cilinder having radius 0.005 and height 0.1, and as a single point for what concerns the fluid flow.

This last assumption is an approximation that does not model the wake region behind the seed, but will give a rather good approximation for the thermal field (that is of main concern in this analysis).

The initial assumed field conditions are relative to the zero-g purely diffusive regime, that corresponds to a quiescent flow field and to a thermal field as per Fig.2.

The assumed axisymmetry of the problem is preserved by setting $i_\vartheta = i_x$, i.e. by assuming that the gravity vector acts along the cylinder's symmetry axis.

3.2 Description of the numerical code

The code used for the numerical experimentations is described in details in [3] and [4].

The code solves the full Navier-Stokes Equations for unsteady problems in two dimensional problems (plane and axysimmetric geometries) with constant and variable mesh option.

The system of equations are discretized with finite difference approximations and then solved with a semi-implicit technique. By denoting by (N+1) the time level at the current step, the non linear convective terms are considered at the time level (N) and written with a second order upwind formulation, whereas the diffusive terms are considered at the time level (N+1) and discretized with central difference formulas. The resulting system of algebraic equationa is then solved with a Gauss-Seidel method. The pressure equation is solved (if required) with the Briley method.

In order to validate the boundary conditions assumed on the central seed, for few cases, the results obtained with the present code were compared with the corresponding ones obtained by a VOF codes (primitive variable formulation) with the correct flow condition of the seed.
The results compare quite well for what concerns the temperature and the flow fields, obviously discrepancies were found relatively to the heat fluxes on the seed's surface.

3.3 Parameters for the evaluation of the g-disturbances

The problem was discretized with a 11x21 grid points mesh, the pressure field option was not implemented.

The following set of parameters was used:

$$Ec = 0 \; ; \; Str = 1 \; ; \; R/L = 0.5 \; ; \begin{cases} Re = 1 & ; \; Pe = Re \\ Re = 1/Pr & ; \; Pe = 1 \end{cases}$$

i.e the viscous dissipation term in the energy equation was discarded, the reference time was assumed to be:

$$tr = Lr \; / \; Vr$$

and the reference velocity was assumed to be, in the two

cases:

$Vr = \nu_g / Lr$ (Re=1) ; $Vr = \alpha_g / Lr$ (Re=1/Pr)

Most of the runs were made by considering a reference length Lr=10[cm] and Pr=6.9 (acqueous solution for which Vr = .001 [cm/s] ; tr = 10.000 [s] in the Re=1 case)

In order to measure the effects produced by the g-disturbances, some norms are used for the measurement of the effects:

a. FLOW DISTORTION PARAMETERS:

$-\psi max$, as the maximum normalized value of the stream function induced in the field by the effect of the buoyancy;

-V max, as the maximum normalized value of the velocity induced in the field by the effect of buoyancy.

Both such parameters allow a direct evaluation of the fluidynamic disturbance with respect to the quiescent reference state.

b. TEMPERATURE DISTORTION PARAMETERS:

- Average Temperature Distortion (D):

$$D\theta = \sum_{i=1}^{N} |(\vartheta - \vartheta_s)|$$

- Maximum Temperature Distortion (Dm):

$$Dm = \max_i |(\vartheta - \vartheta_s)|$$

where: N is the number of grid points,
ϑ is the local nondimensional temperature
ϑ_s is the local nondimensional temperature at the reference quiescent state (@ g=0)

The evaluation of the temperature disturbance is very dependent upon the specific experiment. The parameters above defined represent a quite good evaluation criteria for the microgravity processing phenomena. In some case probably the measure of the distortion of surface heat fluxes can be also valuable, but such measure is out of the scope of the present analysis.

4. RESULTS OF THE NUMERICAL EXPERIMENTS

4.1 Quasi steady acceleration field

The effects of a quasi steady acceleration field

deriving from the residual gravity along the cylinder axis has been computed in order to define a treshold limit for acceptability in manned Space Station investigations.

By considering the fluid to be a water solution, and by assuming a $\Delta(T) = 16[K]$, we have considered two gravity levels:

$$g = 10^{-5} g_0 \quad ; \quad g = 10^{-6} g_0$$

The correspondig values of the Grashof numbers are :

$$Gr = 800 \quad ; \quad Gr = 80$$

The code extimates for such two cases the following values of the disturbance parameters above defined:

g/g	Gr	Vmax	Ψ_{max}	D_ρ	D_m
10^{-5}	800	19.6	.247	4.6	.202
10^{-6}	80	1.94	.0243	.49	.0233

As expected the values of the disturbance parameters are almost proportional to the Gr, and the system acts as a linear one.

Since it is evident that the residual gravity field is a disturbance that cannot be avoided, it may be rewarding to compare the distortion parameters of all the other disturbances with those above computed. The g-jitters that induce distortion parameters of the same order of those corresponding to the residual gravity level of $g/g_0 = 10^{-6}$ (Gr=80) can be accepted whatever is the particular fluid experiment to perform in space.

In such manner we define a general treshold limit for acceptability in manned Space investigations.

4.2 Single Pulses g-jitters

These disturbances may result from forces external to the S/C system.

The time profiles of such single pulses are square single waves with varying magnitude (Gr) and duration (tp).

Most of the experimentation was devoted to the understanding of the behaviour of the effects generated

into the fluid, during the forced phase and the following relaxation phase.

Figg.3,4,5 refer to the three different profiles:

g/g	Gr	tp[s]
$.5 \cdot 10^{-3}$	40,000	4
10^{-3}	80,000	2
$2 \cdot 10^{-3}$	160,000	1

The motivation of these experiments is self evident: verification of the dependence of the disturbance parameters upon the mechanical energy transfered to the fluid (the product [Gr · tp] being constant).

The results can be summarized as follows:

- for small values of tp the system can be treated as linear in the forced phase;
- the fluid parameters grow within the forced phase with a ramp proportional to Gr and reach peak values proportional to the product [Gr·tp], after they decay to zero;
- the thermal parameters grow within the forced phase with a ramp proportional to the product [Gr·tp], with a delay time almost proportional to tp/2, after they continue to grow.

The behaviour of the parameters in the relaxation phase is shown in Fig.5.

The fluid parameters decay with a characteristic decay time of about 50[s] (about 1/200 of the reference viscous time).

The thermal parameters show an exponential growth, reaching a maximum at 70[s] for Dm and at 150[s] for D_ρ. After the relaxation process takes place with a decay time of the order of 220[s] for D_ρ and of the order of 300[s] for Dm.

The major issue is the growth of the thermal disturbances also after the end of the g-pulse.

Further investigations made with different values of the Pr number lead to conclude that such thermal characteristics times (for the growth, for the maxima, and for the decay) depend mostly on the viscous characteristic time.

The main conclusion of such numerical experiment is that for time pulses small enough with respect to the

viscous time the following correlations apply:

$$\hat{Vm} = 0.6\ Gr\ tp^{4} / Re^{2}$$
$$Dm = Gr\ tp^{6} / Re / 111.8$$

By assuming as treshold limits the values generated by a residual gravity field of 10 g ($\hat{Vm} = 2$; Dm = .02), we can correlate the suggested limiting curves in the g-tp plane as follows:

fluid limit : $g/g_o = (0.333 \cdot d / Lr / \beta_T / \Delta T / g_o) / tp$
thermal limit : $g/g_o = (2.237 \cdot \nu / Lr / \beta_T / \Delta T / g_o) / tp$

Such curves are plotted in Fig.6 in a g/g_o versus 1/tp graph for the case of water solution with a ΔT=16[K]. As it can be noticed, for the case of interest, the thermal limit is less restrictive that the fluid limit.

4.3 Double pulses g-jitters

4.3.1 Compensated double pulses

These disturbances may result from causes internal to the S/C. Their magnitude is of the order of 1 mg .

The assumed shape of the g-jitter correspond to a positive square profile followed by a corresponding negative square profile after a delay time (td).

Figg.7,8 consider the case of td=0 with a Gr=80,000 ($1mg_o$) and tp=1[s], they show the disturbance parameters during the forced phase and the immediately following relaxation. As expected the behaviour during the forced positive period (0<t<tp) the behaviour is exactly the same as the single pulse, but when the negative pulse comes (tp<t) the velocity disturbance reduce practically to zero and the temperature parameters do not show any overshooting since the relaxation phase is immediately activated.

Figg.9,10 refer to the relaxation phase in the case of variable delay time.

The behaviour of the fluid parameters confirms the expectation : the maxima occur at the end of the first positive pulse.

The thermal parameters show a different trend

due to their different growth after the first pulse: the overall disturbance is minimized if the delay time is small with respect to characteristic time of the thermal growth.

Figg.11,12 refer to the very interesting case of two immediately subsequent pulses that compensate each other, but have different shape with the same global energy. The behaviour of the graphs confirm the linearity of the system with respect to the mechanical energy feeded in.

Saw-toothe profiles used by NASA for describing the crew motion induced g-jitter [5] have been experimented and the results are pratically fully correlable by equivalent square profiles.

4.3.3 Definition of limiting curves for compensated double pulses

The limiting curves for internal disturbances may be easely defined by using the result of the numerical experiments and the correlation given in para 4.2 for single pulses.

The limiting curves are easely derived and presented in Fig.13. Obviously in this case the fluid limit is determined by the first pulse, whereas the thermal limit is decreased if the delay time is much less than the time for maximum of the thermal parameter.

4.4 Subsequent pulses with the same sign

Two subsequent pulses with the same sign and with a time interval could be generated by external causes.

The motivation of such experiment derives by the willing to show that grouth of the thermal parameters, also after the end of the g-pulse, can cause a strong amplification if another pulse of the same sign is applied when the thermal parameter nearly reach its maximum.

Figg.14,15 show that with a delay of about 150[s] the fluid parameters present almost the same overall maxima, whereas the thermal parameters exhibit maxima almost two times those generated by single pulses.

5. CONCLUSION

A review of the tolerable g-level criteria has shown that, even for a well defined class of experiments the g-f curves typically prescribed by the Agencies for orbiting platforms, is actually based on a dangerous oversimplification of the causes/effects on board.

It has been showed that periodic g-jitters are probably the least dangerous for the experiments, and that single or double pulse jitters may cause much severe disturbances.

The results of the numerical experiment clearly demonstrate that the effects of the velocity, on the thermal, and on the concentration fields may be substatially different because of the relative characteristics times.

Moreover as per the damped mechanical system a sort of resonance effect can be created by external causes.

Finally great relevance appears to have the conclusion that the effect of a negative pulse following a positive one does not cancell the thermal effects of the previous one. This non linear phenomenon deserves detailed further investigations.

6. REFERENCES

1. MONTI,R.;LANGBEIN,D.;FAVIER,J.J.: "Influence of residual Accelerations" - Ch.XIX of the "In Orbit 2000" - ESA Pubbl. - in print

2. HAMACKER;JILG;MERBOLD: "Analysis of Microgravity measurements performed during D-1" - 6th European Symposium Material Sciences under Microgravity Conditions - Bordeaux, Dec.1986

3. GOLIA,C. et alia : "Transient development of Marangoni Flows", l'Aerotecnica Missili e Spazio,Vol.64,N.3,pp.186-191,1985

4. GOLIA,C. et alia : "Effects of Variable Transport Properties on Thermal Marangoni Flows", Acta Astronautica, Vol.13,N.11/12,pp.661-667,1986

5. KNABE,W.,EILER,D. : "Low-Gravity Environment in Spacelab", ERNO Report 1986

6. TechnoSystem Report : "Tolerable G-level for Fluid Science Experiments" TS-7-87, Aprile 1987

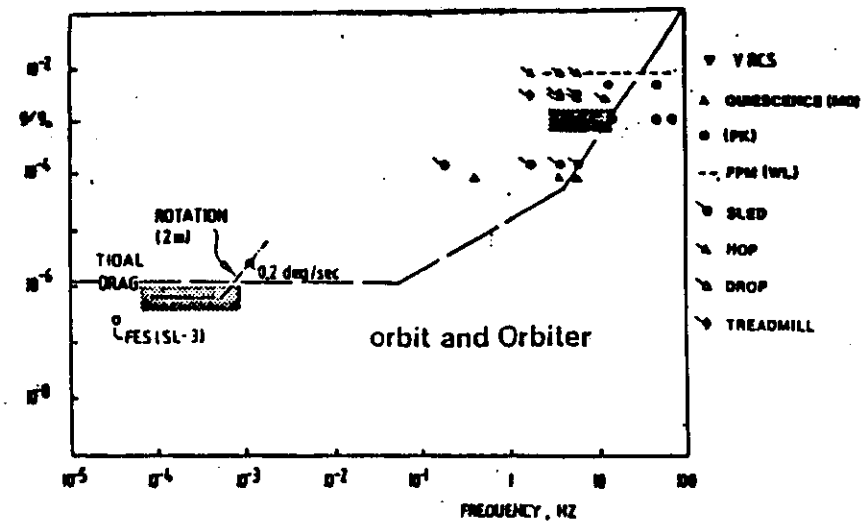

Fig.1 - Summary of measurements results

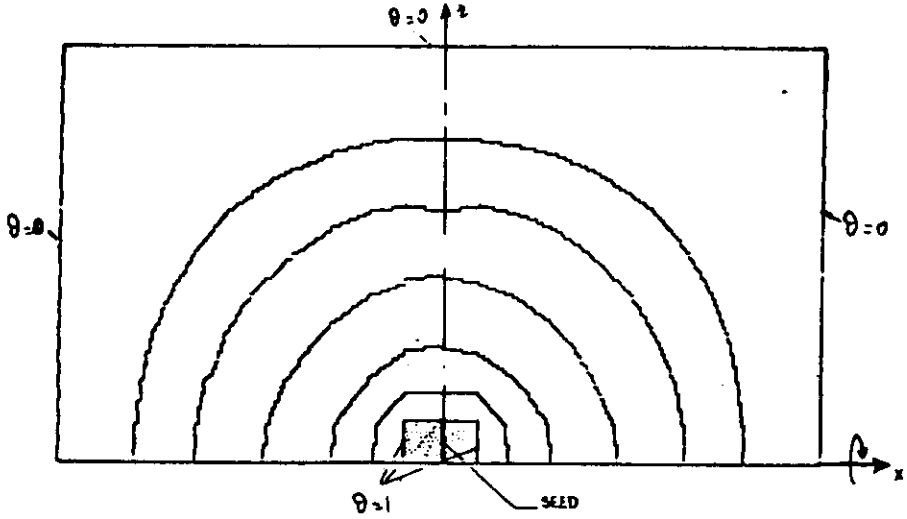

Fig.2 - Isotherms at steady conditions - Reference state g=0

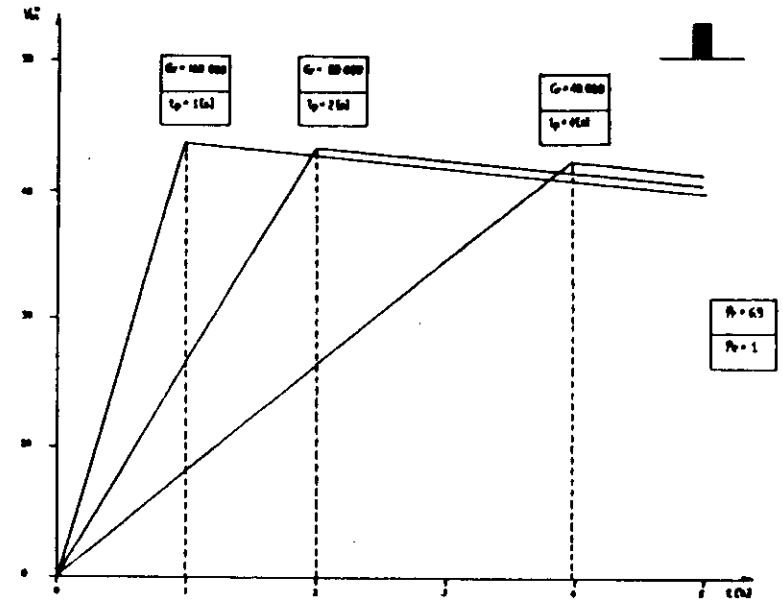

Fig.3 - Velocity distortion parameters for single pulse of different duration but equal impulse

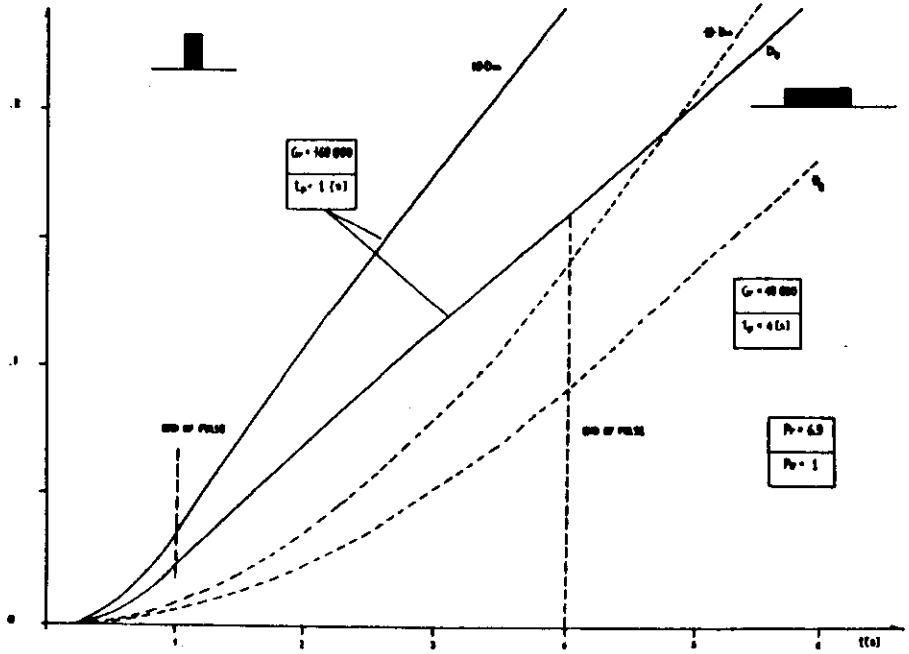

Fig.4 - Thermal distortion parameters evolution for equal impulse disturbances

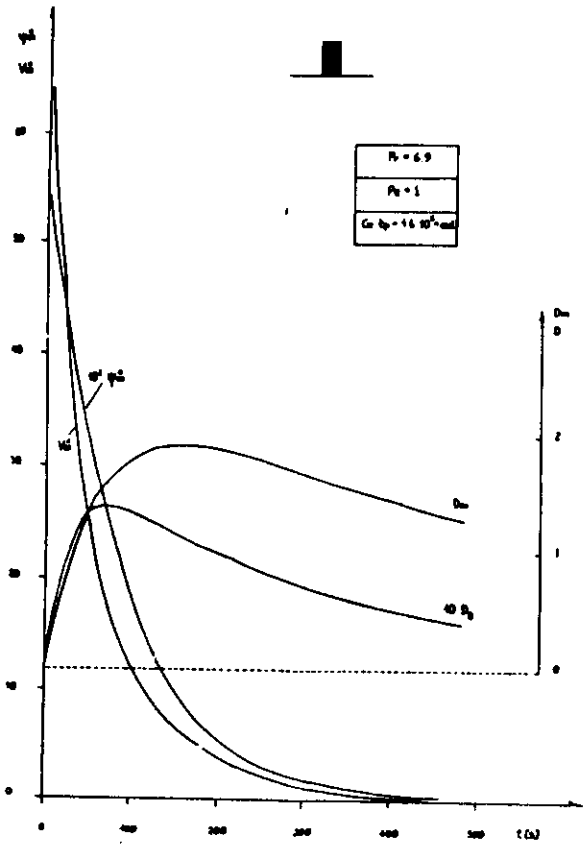

Fig.5 - Distortion parameters time profiles

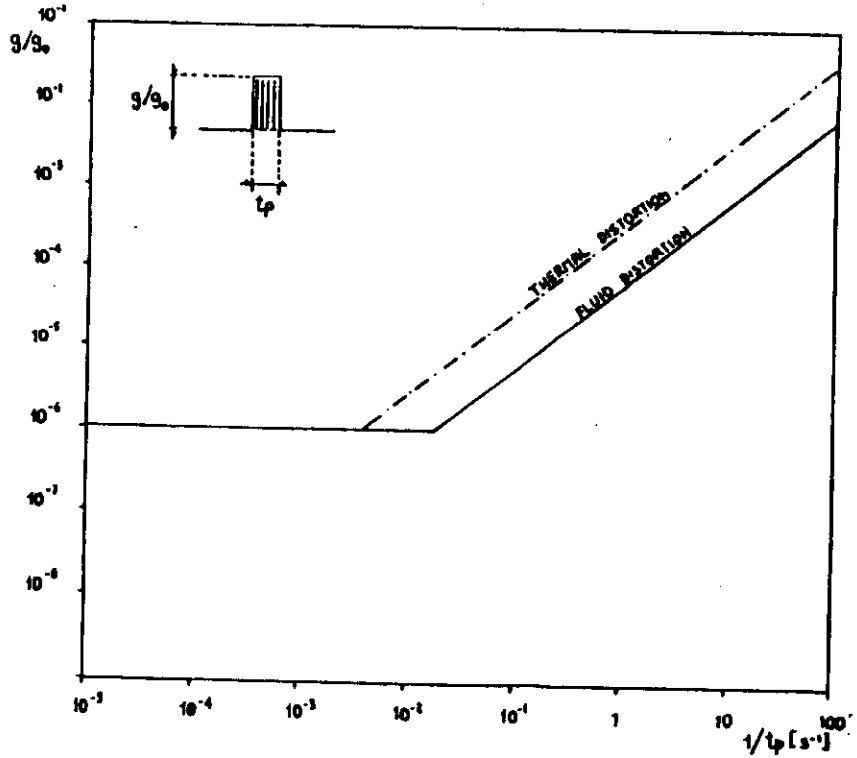

Fig.6 - Tolerable single pulse g-level versus the inverse of the pulse duration

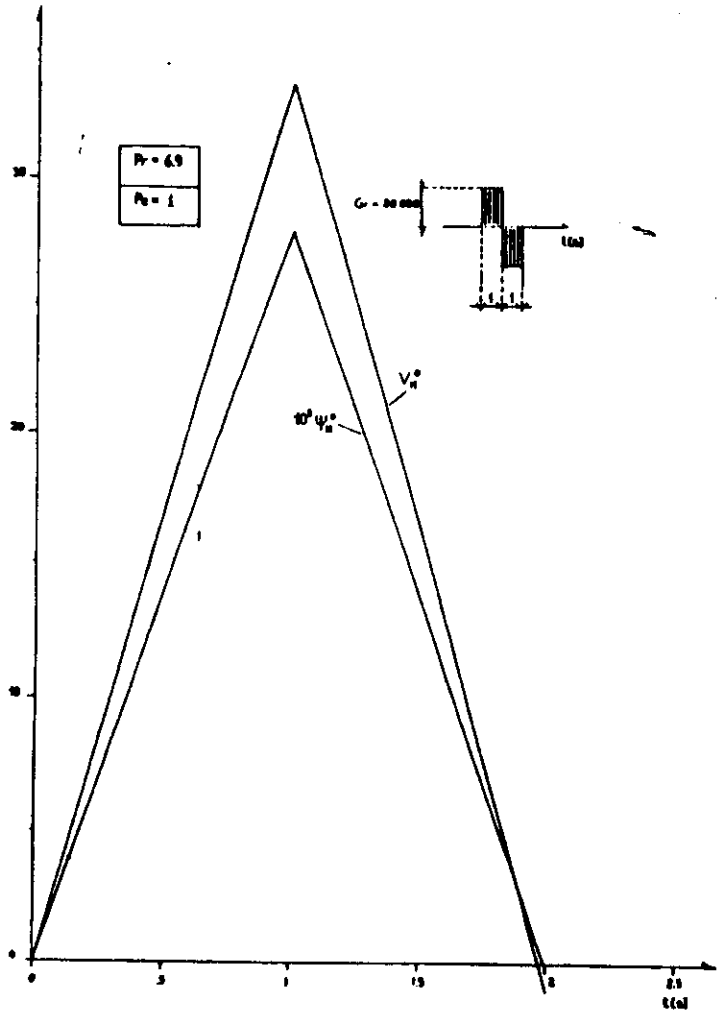

Fig.7 - Double pulses : time profiles of the distortion parameters

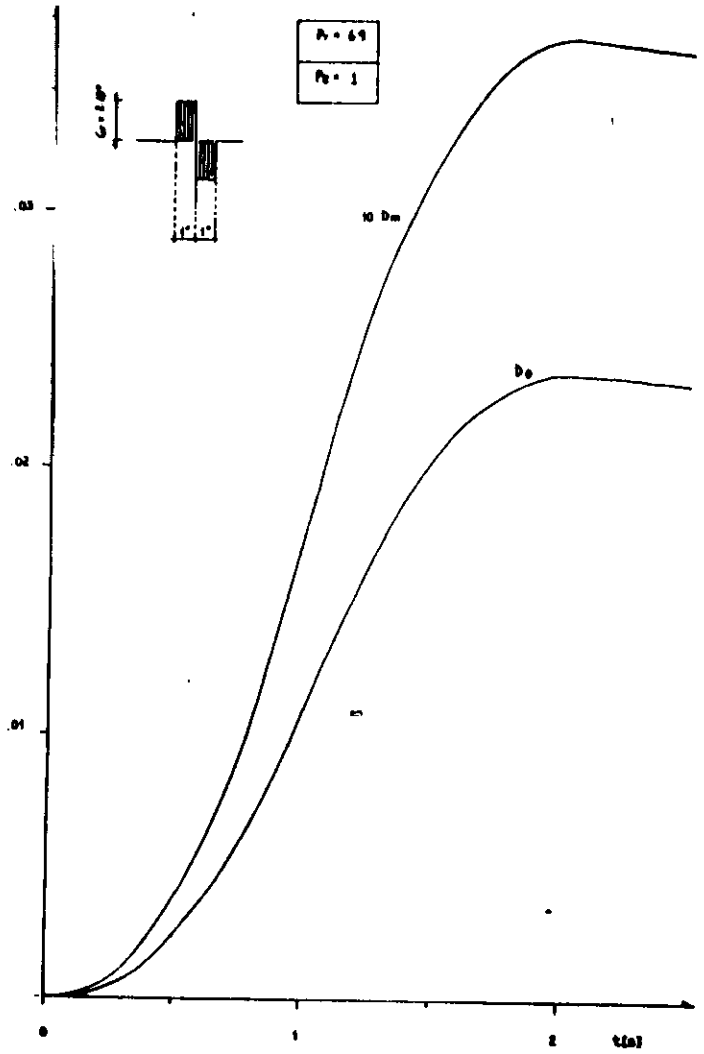

Fig.8 - Double pulses : time profiles of the distortion parameters

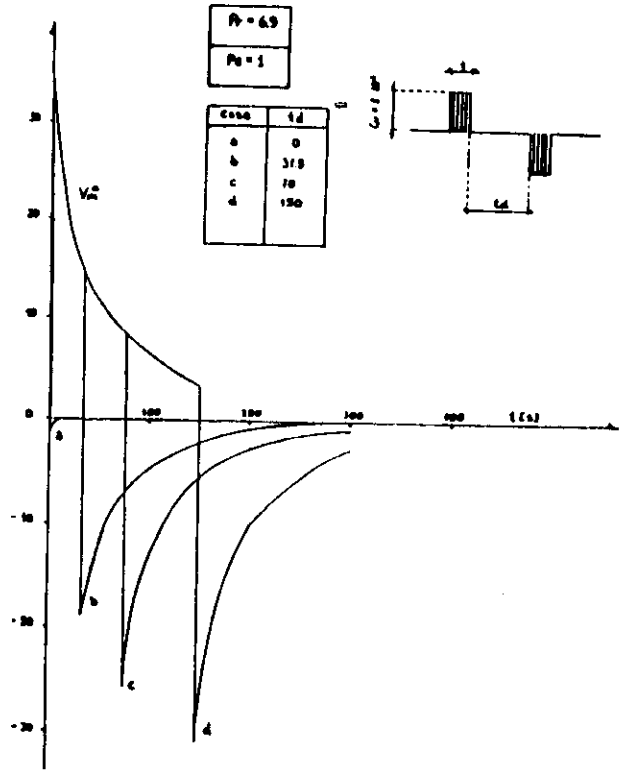

Fig.9 - Velocity distorsion parameter time hystory for double pulses

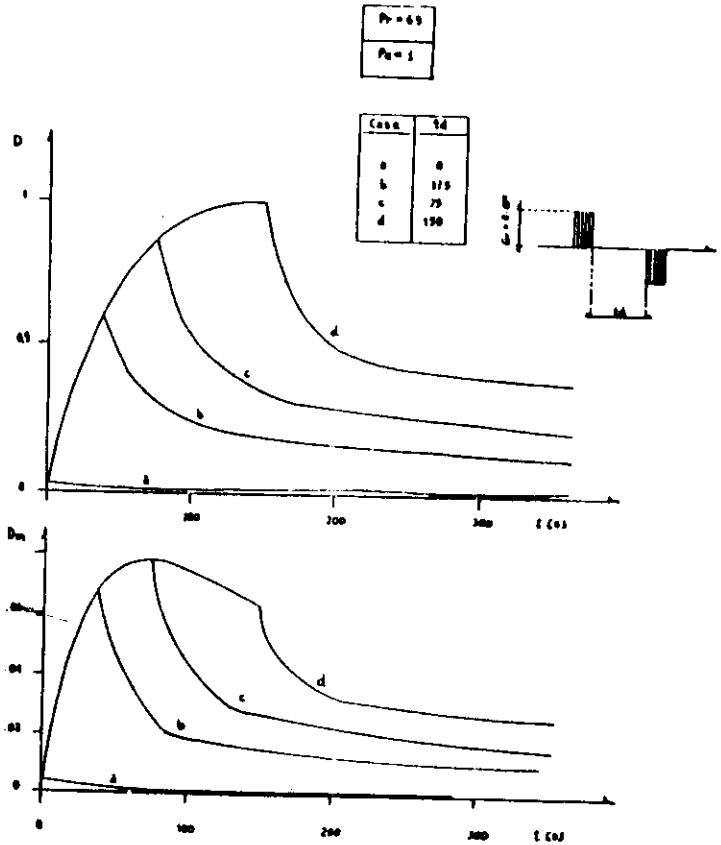

Fig.10- Thermal distortion parameter time hystory for double pulses

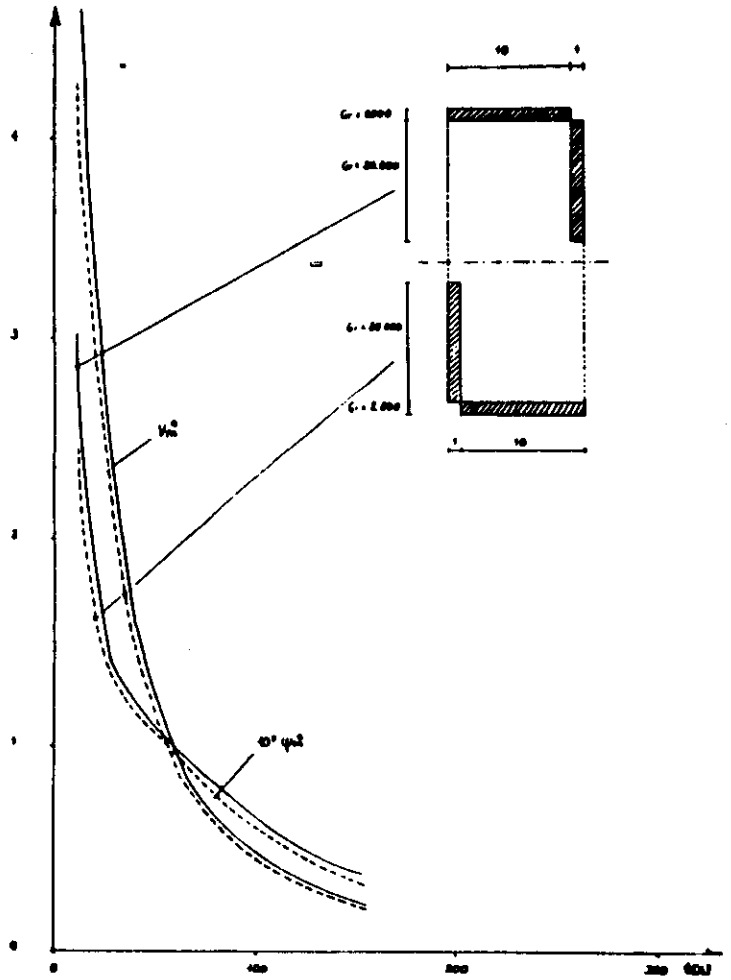

Fig.11- Velocity distorsion parameter
Inequal pulses same impulse

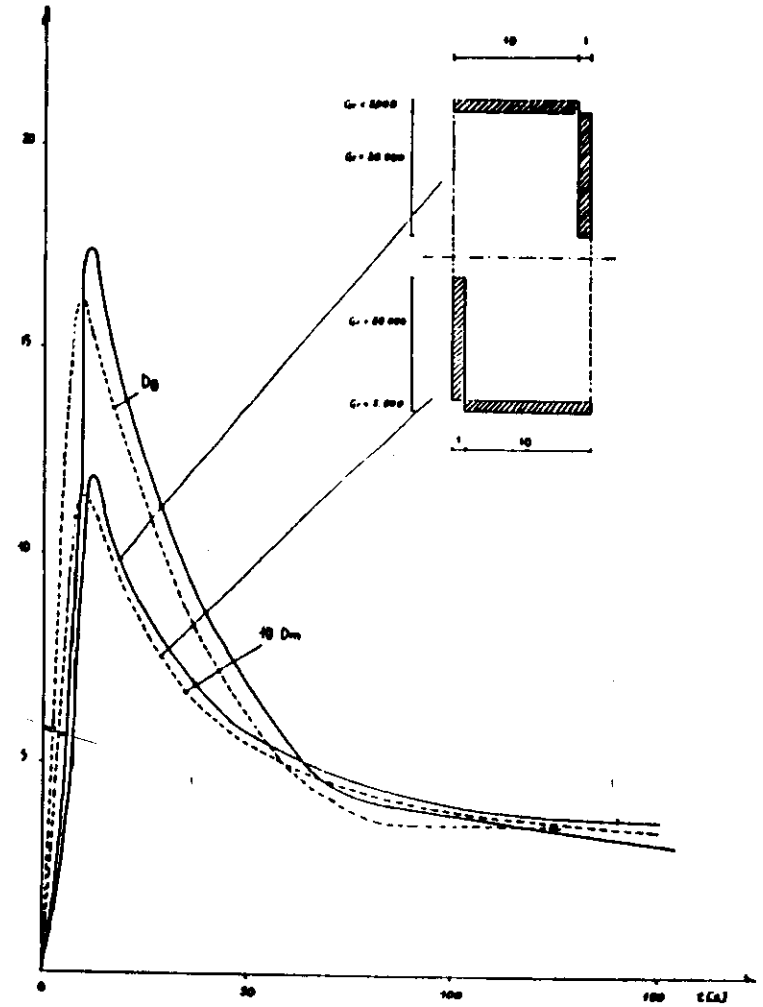

Fig.12- Thermal distortion parameters
inequal pulses same impulse

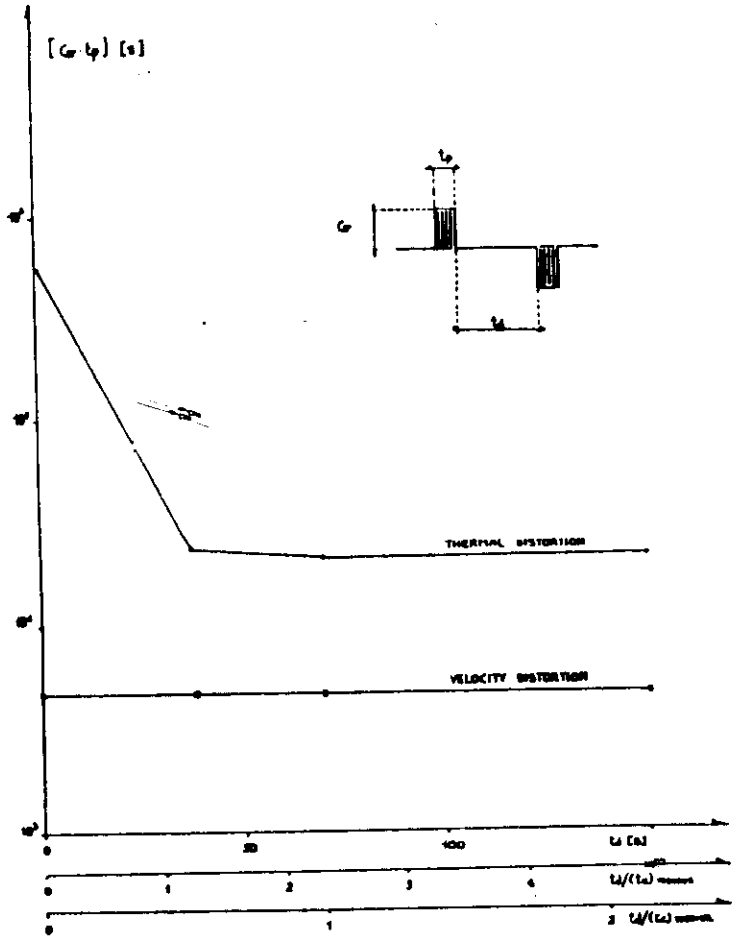

Fig.13- Tollerable impulse [Gr tp] for double pulses versus time delay [td]

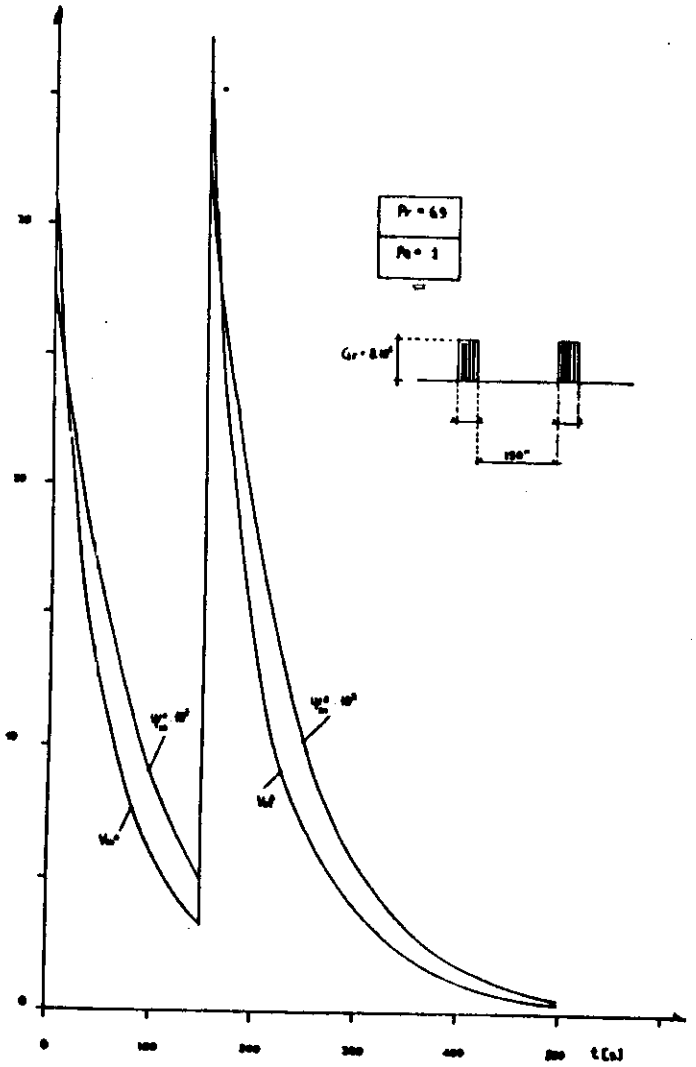

Fig.14- Fluid distorsion parameters for double positive pulses

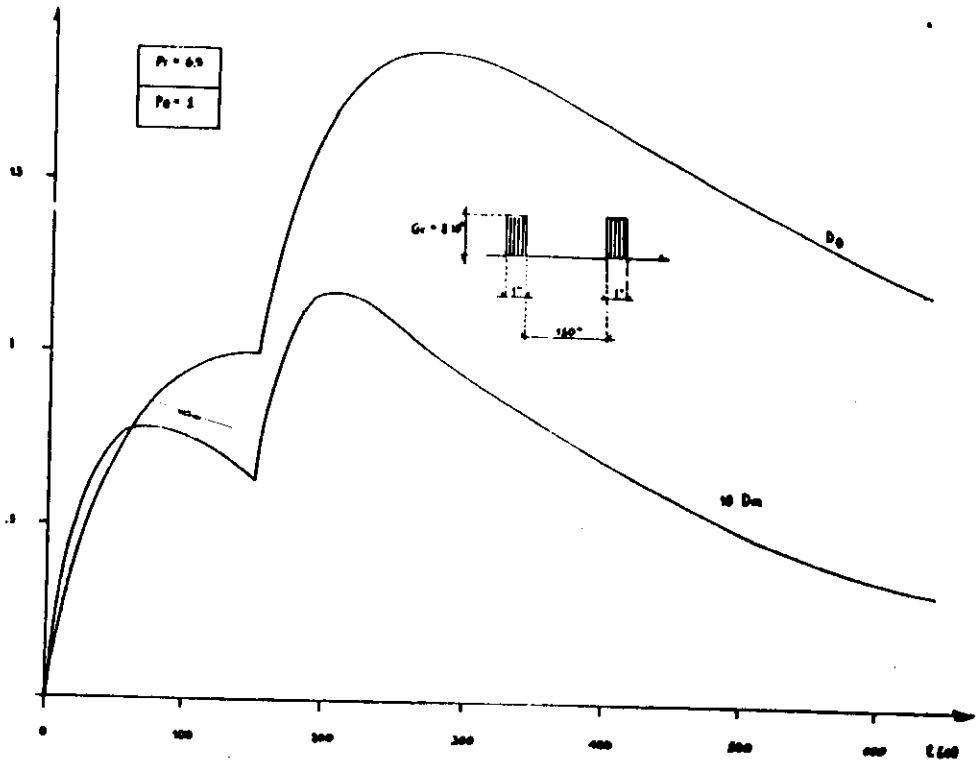

Fig.15- Thermal distortion parameters for double positive pulses

DRAFT

ON THE EFFECTS OF THE IN ORBIT ACCELERATION ON MICROGRAVITY EXPERIMENTS IN FLUIDYNAMICS

R. MONTI - C. GOLIA
Istituto di Aerodinamica "U. Nobile"
Università di Napoli

IX CONGRESSO NAZIONALE DELLA
ASSOCIAZIONE ITALIANA DI AERONAUTICA ED ASTRONAUTICA

PALERMO 28-28 OTTOBRE 1987

ON THE EFFECTS OF IN ORBIT ACCELERATION ON
MICROGRAVITY EXPERIMENTS IN FLUIDYNAMICS

R.Monti - C.Golia
Istituto di Aerodinamica "Umberto Nobile"
Universita' di Napoli

Summary

The effects produced by the various types of g-disturbances occurring during manned space missions in fluid science microgravity experiments are evaluated through extensive numerical experimentations with a code solving the full set of Navier-Stokes Equations.

Parameter norms to measure the fluid and the thermal disturbance effects, and new criteria are then proposed for the evaluation of the maximum acceptable g-fields on microgravity platforms for fluid experiments in terms of the various typologies of the g-jitters.

1. INTRODUCTION

Microgravity experimentations on space platforms are obviously motivated by the need of a quiet, very low g-environment. An ideal Microgravity Environment (MG) is a real zero-g that does not appear feasible in LEO Spacecrafts mainly because of the air drag, S/C manoeuvres, rotating machinery on boards, and, when present, crew activity.

Latest recording on the g-field on board of manned dedicated missions show how g-disturbances of random nature (g-jitters) exhibit relatively large peaks (of the order of 10^{-2} g) that may affect a number of microgravity experiments.

The evaluation of the effects of those g-disturbances on different classes of experiments is of paramount importance for the experimenters, for the payloads manufacturing companies and for the Space Agencies that must specify the requirements on the "allowable" g-levels (or g-fields) for the S/C on which the Microgravity Experiment takes place.

Following the work reported in [6] we review the previous criteria of the allowable g-levels (e.g. as specified by ESA for unmanned platforms like EURECA) and